nature chemical biology

Progressive ordering with decreasing temperature of the phospholipids of influenza virus

Ivan V Polozov[1], Ludmila Bezrukov[1], Klaus Gawrisch[2] & Joshua Zimmerberg[1]

Using linewidth and spinning sideband intensities of lipid hydrocarbon chain resonances in proton magic angle spinning NMR spectra, we detected the temperature-dependent phase state of naturally occurring lipids of intact influenza virus without exogenous probes. Increasingly, below 41 °C ordered and disordered lipid domains coexisted for the viral envelope and extracts thereof. At 22 °C much lipid was in a gel phase, the fraction of which reversibly increased with cholesterol depletion. Diffusion measurements and fluorescence microscopy independently confirmed the existence of gel-phase domains. Thus the existence of ordered regions of lipids in biological membranes is now demonstrated. Above the physiological temperatures of influenza infection, the physical properties of viral envelope lipids, regardless of protein content, were indistinguishable from those of the disordered fraction. Viral fusion appears to be uncorrelated to ordered lipid content. Lipid ordering may contribute to viral stability at lower temperatures, which has recently been found to be critical for airborne transmission.

Membranes of most enveloped viruses form by budding out from the plasma membranes of their host cells a highly select subset of plasma membrane components. In general, the selected membrane proteins are coded by the viral genome, whereas lipids are recruited from host membranes; however, the lipid composition of the viral envelope differs from that of the host membrane[1,2] and from other budding viruses[3]. The envelope of influenza contains higher amounts of both cholesterol[1] and glycosphingolipids[4]—lipids known to partition into the liquid ordered (l_o) phase. The l_o phase is characterized by extended hydrocarbon chains having a reduced gauche-*trans* isomerization compared with those of the liquid disordered (l_d) phase, but having a similar rotational and translational mobility[5]. Liquid ordered phases are thought to be at the core of lipid rafts[6], which are defined as transient membrane microdomains that are enriched in sphingolipids and cholesterol (**1**)[7]—a hypothesis that has generated much debate[8,9].

The influenza virus has played a pivotal role in the development of the raft hypothesis, starting with early studies that inferred ordered domains using spin probes[10–12] and fluorescence[13,14] and that suggested that an ordered lipid domain is selected *in toto* as the envelope during budding from the plasma membrane[15]. These lipids are either selected at the time of budding or pre-selected as the 'pre-envelope' suggested by clusters of the viral envelope protein hemagglutinin seen in immunoelectron microscopy[16].

Although detection of virus-sized domains of lipids (~100-nm diameter) is below the limit of resolution of fluorescent microscopy, large micrometer-sized membrane domains are reliably detected[17–19]. Recently, proton magic angle spinning NMR (^{1}H MAS NMR) has been used to determine the phase diagram of the same lipid compositions used to study large membrane domains in lipid bilayers and other membranes, along with compositional information on each phase[20–22]. By spinning membrane samples rapidly at the magic angle (54.7°) to the magnetic field, one overcomes a severe limitation: broadening of NMR resonances by dipolar interactions, which results in a loss of resolution such that there is only a single unresolved hump. Application of ^{1}H MAS NMR to studies of lipid membranes is possible because the intrinsic fast axial reorientation of lipids yields proton resonances that are broadened inhomogeneously, which allows restoration of resolution at relatively low spinning frequencies[23]. The ^{1}H MAS NMR resonance linewidth of the spinning centerband and sidebands is sensitive to the rate of gauche-*trans* isomerization of lipid acyl chains and axial reorientation; thus, it can be quantified as a measure of different states of lipid membranes[20,21]. At a spinning frequency of 10 kHz, the characteristic linewidth of the methylene resonance of saturated hydrocarbon chains in ^{1}H MAS NMR spectra is 25–100 Hz for lipids in the l_d phase, 500–1,000 Hz in the l_o and larger than 1.5 kHz in the solid ordered (s_o) gel state, in which lipids are packed in a crystalline lattice with extended chains and severely restricted lateral and rotational mobility. The ^{1}H MAS NMR spectrum consists of a centerband flanked by sidebands spaced at multiples of the spinning frequency (10 kHz corresponds to 20 ppm at the magnetic field strength of 11.7 T). Absolute values of sideband/centerband intensity ratios are dependent on the average order in the membrane and thus provide an additional characteristic of the system that is similar to the order parameter derived from deuterium NMR (refs. 21,24). The ratio of sideband/centerband intensities depends on sample composition and must be determined individually for each lipid, but at 10 kHz spinning frequency generally it is in the range of 0–0.04 for the l_d phase, 0.05–0.12 for l_o and 0.1–0.2 for s_o

[1]Laboratory of Cellular and Molecular Biophysics, National Institute of Child Health and Human Development, 10D14, 10 Center Drive MSC 1855 and [2]Laboratory of Membrane Biochemistry and Biophysics, National Institute of Alcohol Abuse and Alcoholism, 3N07, 5625 Fishers Lane MSC 9410, National Institutes of Health, Bethesda, Maryland 20892, USA. Correspondence should be addressed to J.Z. (joshz@helix.nih.gov).

Received 27 August 2007; accepted 31 December 2007; published online 2 March 2008; doi:10.1038/nchembio.77

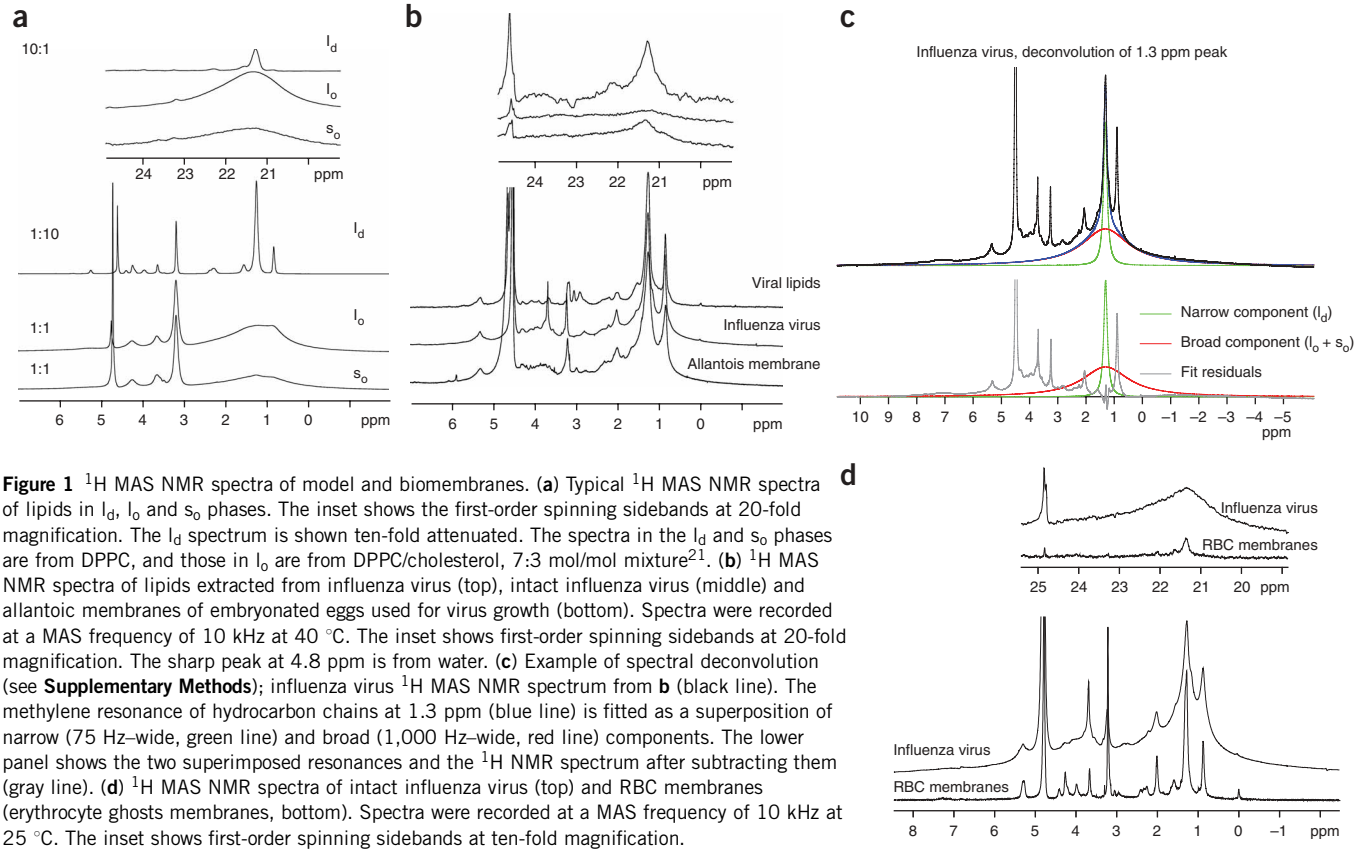

Figure 1 ^{1}H MAS NMR spectra of model and biomembranes. (**a**) Typical ^{1}H MAS NMR spectra of lipids in l_d, l_o and s_o phases. The inset shows the first-order spinning sidebands at 20-fold magnification. The l_d spectrum is shown ten-fold attenuated. The spectra in the l_d and s_o phases are from DPPC, and those in l_o are from DPPC/cholesterol, 7:3 mol/mol mixture[21]. (**b**) ^{1}H MAS NMR spectra of lipids extracted from influenza virus (top), intact influenza virus (middle) and allantoic membranes of embryonated eggs used for virus growth (bottom). Spectra were recorded at a MAS frequency of 10 kHz at 40 °C. The inset shows first-order spinning sidebands at 20-fold magnification. The sharp peak at 4.8 ppm is from water. (**c**) Example of spectral deconvolution (see **Supplementary Methods**); influenza virus ^{1}H MAS NMR spectrum from **b** (black line). The methylene resonance of hydrocarbon chains at 1.3 ppm (blue line) is fitted as a superposition of narrow (75 Hz–wide, green line) and broad (1,000 Hz–wide, red line) components. The lower panel shows the two superimposed resonances and the ^{1}H NMR spectrum after subtracting them (gray line). (**d**) ^{1}H MAS NMR spectra of intact influenza virus (top) and RBC membranes (erythrocyte ghosts membranes, bottom). Spectra were recorded at a MAS frequency of 10 kHz at 25 °C. The inset shows first-order spinning sidebands at ten-fold magnification.

(values are respectively 0.0025, 0.11 and 0.12 for l_d, l_o and s_o; examples shown in **Fig. 1a**). For samples with coexisting membrane domains, the centerband of the ^{1}H MAS NMR spectrum is dominated by narrow peaks from the l_d phase, whereas broad components from the ordered phases are markedly pronounced in the sideband region of the spectrum. Moreover, ^{1}H MAS NMR with application of pulsed magnetic field gradients enables measurement of lipid diffusion rates in membranes[25] and of fluid domain sizes[20]. Here we apply these techniques to test the hypothesis that ordered lipids exist in the envelope of the influenza virus. We also measured membrane fusion of virus to cells to probe the biological significance of the viral envelope ordered domains. We find that the lipids in the viral envelope are indistinguishable from lipids in the l_d phase at temperatures above ~40 °C, with an increasing fraction of ordered lipids at increasingly colder temperatures.

RESULTS

Coexistence of lipid domains at room temperature

As a point of reference, **Figure 1a** shows the spectra of pure s_o, l_o and l_d phases of 1,2-dipalmitoyl-sn-glycero-3-phosphocholine (DPPC; **2**) plus cholesterol mixtures. Spectra of intact influenza virus were compared to spectra of extracted lipids (**Fig. 1b**). The viral spectra are dominated by resonances from its lipids, as expected for MAS NMR spectra. Because of their slower motions and rigidity, signals from proteins are present as extremely wide bands—for example, the amide protons in the range of 7–10 ppm. The most intense lipid peak is from methylene resonances of hydrocarbon chains (1.3 ppm). At 36 °C and below, this peak displays a non-Lorentzian shape characteristic of coexisting environments of differing order[20]. A single Lorentzian line at 20% of maximum intensity is only twice as wide as at half-height. The substantial width at the base of the methylene peak in the viral spectra (**Fig. 1b**) is thus indicative of the presence of another broad spectral component. We determined at least two superimposed components (**Fig. 1c**); the narrow one (75 Hz linewidth) is from lipid in the mobile l_d, and the broad component (1 kHz) is from lipids in ordered domains l_o and/or s_o (distinguishing of l_o and s_o is difficult from a single spectrum; we address this issue further below). The broad component also has contributions from proteins, RNA and the proton background signal of the NMR probe. The detection of superimposed lipid resonances in a homogeneous viral preparation is clear evidence for coexistence of lipid domains, with a residence time of lipids in those domains on the order of a millisecond or longer (**Supplementary Discussion** and **Supplementary Fig. 1** online). The major difference between the NMR spectra of intact virus, compared to protein-free liposomes of extracted viral lipid, is seen in the spectra of the first-order spinning sidebands (21.3 ppm). The spectrum of intact viruses contains only a broad component, but the protein-free viral lipids contain both narrow and broad components with respective linewidths of ~100 Hz and ~500 Hz (corresponding to 0.2 and 1 ppm at the proton resonance frequency of 500 MHz). The absence of a narrow component in the sideband of the viral spectrum is either due to particularly low-order parameters of lipids in the l_d phase or because of a very rapid decline of rotational echo amplitudes due to diffusional reorientation of lipids within 100 μs, the time of one rotor revolution at 10 kHz spinning frequency. Such reorientation is indeed expected for lipids diffusing in virus-size particles but not in much larger multilamellar vesicles made from viral lipid extracts.

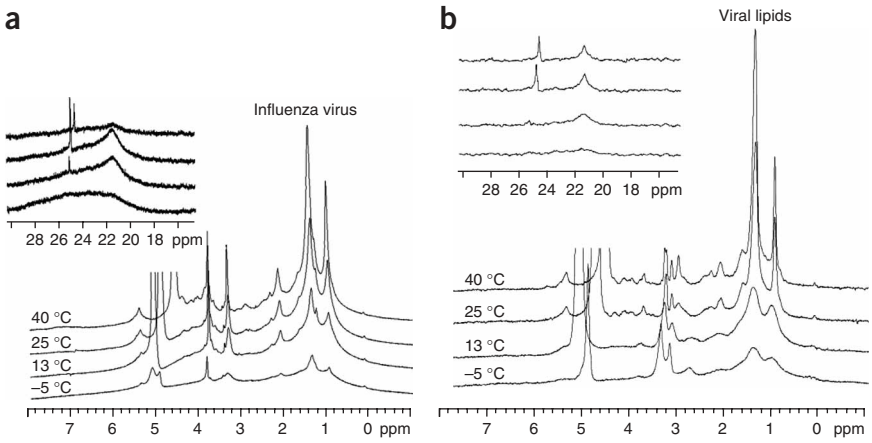

Figure 2 ^{1}H MAS NMR spectra as a function of temperature. (**a**) ^{1}H MAS NMR spectra of influenza virus recorded at 10 kHz at temperatures of 40 °C, 25 °C, 13 °C and –5 °C. (**b**) ^{1}H MAS NMR spectra of influenza virus total extracted lipids recorded at 10 kHz at temperatures of 40 °C, 25 °C, 13 °C and –5 °C. The inset shows first-order spinning sidebands at 20-fold magnification.

Because our viral lipids were derived from cells in the allantoic membranes of embryonated chicken eggs, we compared the spectra of virus and allantoic membranes (**Fig. 1b**). The spectra have a similar resolution and intensity of resonances, despite the fact that the allantoic membrane is a biological tissue. Note that a few minor sharp resonances in these spectra are from water-soluble metabolites. They were distinguished from membrane resonances by NMR diffusion experiments that reflect the much higher diffusion rates of water-soluble substances.

As for viral membranes, the allantoic membrane resonance at 1.3 ppm has a superimposed broad component. This broad signal dominates the intensity of the spinning sideband but is present in the centerband as well. Presence of broad components in the ^{1}H MAS NMR spectra of influenza virus is particularly obvious when spectra are compared to those of human red blood cell (RBC) membranes, which appear to be in the l_d phase above 22 °C. Resolution of RBC spectra at 25 °C (**Fig. 1d**) is comparable to resolution of model membranes in l_d (**Fig. 1a**).

Ordered fraction increases below 40 °C

To estimate the fraction of ordered domains in viral membranes, we recorded ^{1}H MAS NMR spectra as a function of temperature. The signal height of hydrocarbon chain resonances is approximately constant at high temperature. Below a certain onset temperature, signal intensity decreases rapidly with lowering temperature (**Fig. 2** and **Fig. 3a**). About 5 °C below the onset there is indication for conversion of intensity of the narrow resonance characteristic of l_d to the broad resonance characteristic of an ordered lipid phase. Integral spectral intensity over the whole spectral range was approximately constant. The linewidth of the high-temperature resonances as well as the constancy of signal height suggest that above 45 °C all lipids are in the l_d phase. The remaining broad proton resonances are from viral proteins and from the proton background of the probe. An onset of ordered lipid domain formation was observed at 34.7 ± 0.5 °C for allantoic membranes and at 43 ± 1 °C and 45 ± 1 °C for virus and protein-free viral lipids, respectively. Thus it is close for intact virus and protein-free viral lipids, but both are different from allantoic membrane. At temperatures below 0 °C, all membranes are essentially in an ordered state (**Fig. 3b**). When ordered domains are large such that lipids reside in them longer than about a millisecond, signal height of the resonance at 1.3 ppm is an excellent measure of liquid ordered phase content because the linewidth of spectra of ordered phases is about one order of magnitude larger, and their height is one order of magnitude lower. The approximate fraction of lipids in the ordered state was calculated by scaling signal height to the resonance height differences between 45 and –5 °C (**Fig. 3b**). Ordered phase content of viruses and extracted viral lipids is similar down to 4 °C. Furthermore, intact viruses and viral lipids have a higher content of ordered domains than allantoic membranes. For reasons explained in the Discussion and in the **Supplementary Discussion**, the amount of ordered phase near the onset of ordered phase formation could be under- or overestimated.

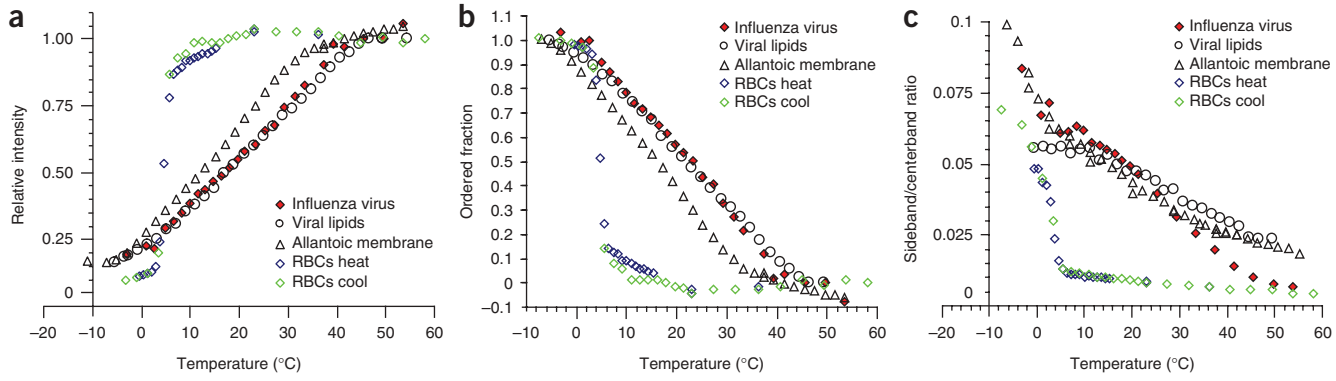

Figure 3 Fraction of ordered lipids as a function of temperature. (**a**) Temperature dependence of the 1.3 ppm resonance of influenza virus, total extracted viral lipids, allantoic membranes and RBC ghost membranes. (**b**) Temperature dependence of the fraction of membranes in ordered domains in influenza virus, viral lipids, allantoic membranes and RBC ghost membranes calculated from the 1.3 ppm resonance height, as explained in the Results. (**c**) Temperature dependence of the ratio of sideband to centerband height of the 1.3 ppm resonance of influenza virus, viral lipids, allantoic membranes and RBC ghost membranes.

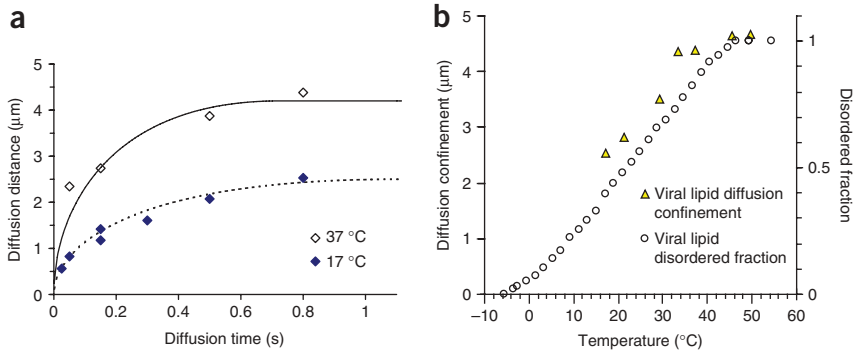

Figure 4 ^{1}H MAS NMR diffusion measurements. (**a**) Time dependence of the average diffusion displacement in viral lipid extract at 37 °C (◇) and at 17 °C (◆). The solid line is a fit with a diffusion rate of 30 μm^2 s^{-1} and diffusion confinement of 4.3 μm. The dashed line is a fit with a diffusion rate of 7 μm^2 s^{-1} and diffusion confinement of 2.5 μm. (**b**) Temperature dependence of diffusion confinement in viral lipid extract. For comparison, the fraction of disordered lipid in viral lipid extract is plotted as well (○, axis on the right).

Lipid extracts form gel-phase membrane domains

The difference in lipid diffusion constants between l_o and l_d (about a factor of three[28,29]) is relatively small, and lipids appear to be able to pass through the boundaries between l_d and l_o phases. Therefore, formation of liquid ordered domains may slow down lipid diffusion but will not produce confinement of lipids to regions smaller than the size of liposomes. In contrast, lipid diffusion in s_o is orders of magnitude slower. Consequently, in the presence of substantial amounts of s_o, when regions of fluid phase domains become discontinuous, spatial confinement of fluid lipids to domains smaller than l iposome size is observed[20]. The latter is detected in a plot of the mean square displacement of lipids as a function of diffusion time.

For comparison, we recorded ^{1}H MAS NMR spectra of human RBC membranes as a function of temperature. Unlike viral or allantoic membranes, lipids in RBC membranes remained in the liquid disordered state until 10 °C, at which point a rapid ordering of lipids ensued with a midpoint of 5 ± 1 °C (**Fig. 3**). Also, in contrast to viral membranes and viral extracted lipids, RBC membranes displayed substantial hysteresis between heating and cooling scans near 10 °C.

Spinning sideband/centerband intensity ratios of the 1.3 ppm resonance are a measure of hydrocarbon chain order parameters[21,24]. In spectra of superimposed ordered and disordered lipid phases, the height of the centerband resonance at 1.3 ppm is primarily determined by contributions from l_d, whereas sideband intensity is determined by contributions from l_o and s_o. Our results are in agreement with lipids in the l_d phase at temperatures above 40 °C and formation of predominantly s_o or l_o at the low temperature end (**Fig. 3c**). The lower ratio in viral membranes compared to viral lipids above 40 °C is probably due to additional lipid reorientation from lipid lateral diffusion in combination with the small size of viruses.

At ambient temperature, spinning sideband/centerband ratio is somewhat higher for viral membranes compared to viral extracted lipid. The difference could be related either to specific protein-lipid interactions or to specific lipid membrane organization—for example, membrane asymmetry, which is known to be conserved in viral membranes long after virus budding from the plasma membrane[26]. To distinguish the effects of membrane proteins from monolayer asymmetry in viral membranes, we investigated reconstituted influenza virus envelopes containing both viral lipids and integral membrane proteins but no matrix proteins or nucleic acids (virosomes)[27] (**Supplementary Discussion** and **Supplementary Fig. 2** online). Virosomes reconstituted from detergent-lipid mixtures lack the membrane asymmetry typical of influenza viral membranes. They displayed formation of liquid ordered phases over the same temperature range as the intact virus (**Supplementary Fig. 3** online), and the protein-free viral lipid liposomes and spinning sideband/centerband ratios were similar as well. Therefore we conclude that thermotropic phase behavior is primarily determined by lipid content, with insignificant contributions from membrane asymmetry and lipid-protein interactions.

At 37 °C the diffusion time dependence of lipid displacement yielded a confinement to 4.3 μm and a diffusion constant of 30 μm^2 s^{-1} (**Fig. 4a**). In the temperature range from 45 to 17 °C, the diffusion constant decreased continuously from 35 to 7 μm^2 s^{-1}. The diffusion confinement remained at 4.3 μm from 45 to 30 °C and decreased continuously to 2.5 μm over the temperature range from 30 to 20 °C (**Fig. 4b**). The 4.3 μm is probably the average radius of liposomes. Confinement of diffusion to a fraction of liposome size at lower temperature suggests formation of a continuous region of a solid ordered phase.

In intact viral particles, lipids appeared immobile as lipid displacement is restricted by the small size of viruses. Their size is below the spatial resolution of the experiment.

To directly test for domain coexistence, we examined giant unilamellar vesicles (GUV) prepared from extracts of influenza virus labeled with rhodamine-dioleoylphosphatidylethanolamine (rhodamine-DOPE; **3**) or Texas Red–dipalmitoylphosphatidylethanolamine (Texas Red–DPPE; **4**). These probes partition preferentially to liquid disordered domains such that membranes have dark (ordered) and bright (disordered) regions[17,18]. Solid-supported multilamellar bilayers were formed by deposition of viral lipids on glass from

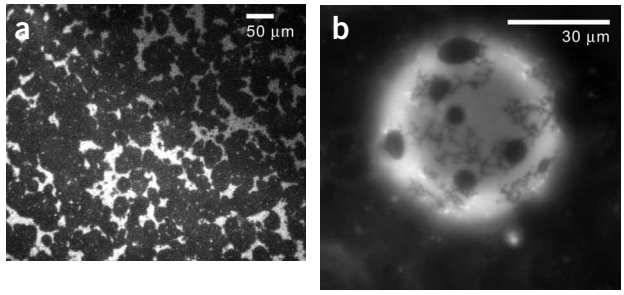

Figure 5 Fluorescence microscopy detection of ordered lipid domains. (**a**) Solid-supported multibilayers of viral lipids containing 1% of Texas Red–DPPE, hydrated at room temperature. (**b**) Ordered and disordered lipid domains coexist on the surface of giant unilamellar vesicles of viral lipids containing 1% of Texas Red–DPPE formed by electroformation on the ITO surface. Vesicle is attached to the surface, forming a hemisphere. Bright area is in the liquid disordered state, while circular dark domains are liquid ordered and dendritic dark domains are solid ordered.

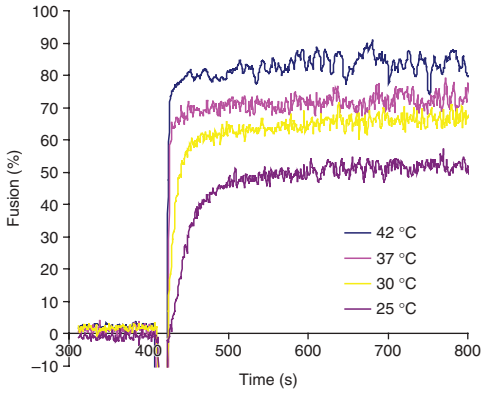

Figure 6 Effect of temperature on lipid mixing assay of influenza virus fusion with RBC membranes. Virus labeled with R18 at self-quenching concentration was mixed with RBC membranes and incubated for 5 min to equilibrate temperature. Fusion was triggered by adjusting the pH to 5 and monitored by the increase of fluorescence intensity due to probe dequenching. Membrane solubilization with 1% Triton X-100 gave complete dequenching, defined as 100% fusion. Decrease in temperature results in a decrease of both the rate and extent of fusion, but fusion is robust at temperatures above 40 °C, where the amount of ordered lipids is negligible.

organic solvent and hydrated at 50 °C. At room temperature the supported bilayers displayed disconnected bright regions and dark regions with noncircular rugged edges characteristic of solid ordered domains (**Fig. 5a**). Addition of excess water to supported bilayers of viral lipid at 50 °C yielded a dispersion of vesicles of variable size and number of lamellae. Electroformation[30] increased the fraction of GUV but did not eliminate vesicle heterogeneity. Occasionally more than two types of domains became visible on the surface of GUV (**Fig. 5b**). At room temperature, some of the vesicles appeared to show l_d-l_o phase coexistence, as judged by the smooth circumference of domains, whereas others displayed a series of morphologically different domains including both circular and dendritic dark domains indicative of l_d-l_o-s_o coexistence. **Figure 5b**, taken at 25 °C, shows 68% of lipid membrane area in l_d (bright area), 11% in l_o, (circular dark domains) and 21% in s_o (dendritic dark domains). Heating of samples decreased the area of dark domains and reduced the contrast between dark and bright domains.

Cholesterol depletion forms gel phase

The egg-grown influenza X31 envelope had a cholesterol content of 53 mol %. To assess the role of cholesterol on domain formation in viral membranes, we incubated virus with (i) methyl-β-cyclodextrin to reduce cholesterol to 1 mol % and (ii) cholesterol-laden methyl-β-cyclodextrin to partially replete to 33 mol % (**Supplementary Table 1** online).

At 37 °C the 1.3 ppm resonance in the center band of ^{1}H MAS NMR spectra is dominated by intensity from lipids in the l_d phase (**Supplementary Fig. 4a** online). Its height did not change with cholesterol content. The most prominent difference between the three samples is the substantially higher intensity of a narrow resonance in the sideband of cholesterol-containing viruses. The higher sideband intensity in the presence of cholesterol is a reflection of the cholesterol-induced increase of lipid order in l_d. The spinning sideband of the 1.3 ppm resonance of cholesterol-depleted virus had the characteristic width of an s_o phase (>95% of spinning sideband intensity was in a 1.76 kHz-wide resonance).

At 4 °C the 1.3 ppm resonance in the centerband of ^{1}H MAS NMR spectra is dominated by contributions from lipids in the l_o and s_o phases. Again, intensity of the residual l_d resonance did not change much with cholesterol content (**Supplementary Fig. 4b**).

Formation of l_o requires the presence of cholesterol. Indeed, according to the width of spinning sidebands, lipids in cholesterol-depleted viruses are not in l_o but are instead in the s_o phase. In contrast, the sideband spectra of both untreated virus and cholesterol-repleted virus suggests coexistence of s_o and l_o phases.

Viral fusion does not require ordered lipids

The above experiments clearly indicate that there would be little or no ordered lipids at temperatures above 40 °C for intact virus. Therefore we tested for fusion of intact virus to cellular membranes at such temperatures. We measured the lipid dequenching that results from lipid dye flux from labeled virus to RBC plasma membrane in the course of membrane fusion induced by lowering pH (**Fig. 6**). Lipid mixing was robust at temperatures above 40 °C. Decreasing temperature from 42 to 25 °C resulted in a decrease of both the rate and extent of fusion, despite an increase in the fraction of ordered lipids in the intact virus. The target membrane is in the l_d state in this temperature range. Thus, ordered domains in viral membranes are not required for virus fusogeneity measured as lipid mixing. The phase state of lipids is not critical for either membrane binding or lipid mixing during influenza hemagglutinin-mediated membrane fusion, although it may play a role in fusion pore development. Though we could not measure fusion pores in the fusion of intact virus, our colleagues used an aqueous fluorescent dye to determine fusion pore opening in the fusion of labeled RBCs to fibroblasts expressing Japan hemagglutinin and found little inhibition of content mixing at 42 °C (and 10% content mixing at 45 °C) (E. Leikina and L.V. Chernomordik, US National Institutes of Health, personal communication). Thus it is unlikely that ordered lipids are required for fusion.

DISCUSSION

The substantial line broadening of ^{1}H MAS NMR lipid hydrocarbon chain resonances from lipid immobilization in ordered phases (l_o and s_o) enables determination of the fraction of ordered lipids in models and biomembranes. We find that phospholipids in viral membranes form ordered lipid phases over a wide range of physiologically relevant temperatures. We have evidence that both l_o and s_o phases coexist with the l_d phase. At 37 °C lipids with broadened spectra (the sum of l_o and s_o phases) represent a minute fraction of the membrane, but at 4 °C almost the entire membrane is in the ordered state. Given that envelope budding occurs at physiological temperature, these data rule out the hypothesis that the influenza envelope is created entirely from an ordered lipid domain[15]. Because the density of envelope protein is near close-packed[31], a majority of the lipid subtending the envelope protein microdomain of the envelope has l_d properties at physiological temperatures. Thus phase behavior cannot explain protein clustering during viral assembly at 37 °C. Yet there must be a selective advantage for the virus to enrich itself in lipids that become progressively more immobile with decreasing temperature. We propose that the palmitoylation of hemagglutinin (maximum of three palmitates per trimer) provides a saturated lipid anchor that may itself induce the collection of other saturated-chain lipids and cholesterol when hemagglutinin is concentrated in the plasma membrane before budding (the viral pre-envelope[16]) for the purpose of increasing viral stability during airborne transmission. Recent super-resolution microscopy studies[32] make clear that hemagglutinin remains mobile within

the pre-envelope, so this concentrated spot of hemagglutinin is not itself a microdomain of gel phase.

One of the advantages of the viral system is the relative ease of isolating a large enough quantity of purified membrane for compositional analysis. Judging from the known phase transition temperatures of individual lipid species, at high temperatures sphingolipids and cholesterol are likely to be at the core of the ordered lipid fraction. At lower temperatures, the increase in the fraction of ordered domains may result from phosphatidylethanolamine (PE) and phosphatidylserine (PS) in the viral lipid matrix. In particular, egg sphingomyelin has a phase transition centered around 39 °C (ref. 33), whereas individual sphingomyelin species melt above 40 °C (ref. 34). PE is known to have a higher gel-fluid phase transition temperature than phosphatidylcholines (PCs) and is likely to convert to s_o. For example, the typical monounsaturated PE species, POPE (**5**) and SOPE (**6**), have midpoints of the main phase transition at 25 °C (ref. 20) and 32 °C (ref. 24), respectively. POPC (**7**) and SOPC (**8**) have transitions below 0 °C and at 6 °C (ref. 21), respectively. Of course, the continuous change of the fraction of ordered lipid with temperature must also result in a continuous change of lipid composition of ordered domains.

Experiments on DPPC plus cholesterol conducted by ^{1}H MAS NMR (ref. 35) and calorimetry[36] show a complex phase diagram above 40 mol % cholesterol, with evidence for gel-l_o phase coexistence at up to 60% cholesterol. Spectral changes that are dependent on cholesterol concentration occur from 45 to 35 °C. It is uncertain whether the latter changes are related to another phase transition or whether they are a reflection of a nonlinear response of an NMR parameter to a continuous change of lipid dynamics. Our spectral simulations assuming rapid exchange of lipids between l_d and l_o (see **Supplementary Discussion**) have shown that the amount of l_o is overestimated when rapid exchange occurs. This is more likely at higher temperature when l_o phase regions are small and lipids diffuse more rapidly. Thus whereas spectral changes of l_o as a function of temperature may yield too little l_o, rapid exchange of lipids between l_d and l_o would yield too much l_o. Therefore near the onset of ordered phase formation, the percentage of ordered phase may not be accurate.

Lipid membranes of influenza viruses were previously studied using fluorescent[13,14] and spin labels[10,11]. The early spin label study of influenza virus[12] aimed only at determination of whether the influenza envelope contains a lipid bilayer, but the study detected less 'fluidity' in the influenza membrane than in the erythrocyte membrane. We confirmed this fact by measuring the ^{1}H MAS NMR spectra of RBC membranes. Such terms as membrane fluidity and rigidity may be obsolete as they ambiguously mask complex lipid behavior and basically reflect high cholesterol content. For example, fluorescent and spin labels are often excluded from the ordered domains, as seen in fluorescent microscopy and through the self quenching of probes on the verge of the transition[18,37,38]. Exclusion of fluorescent groups and spin labels from solid ordered domains may under-report their presence in biological membranes. Furthermore, introduction of fluorescent lipids into live membranes is a nontrivial task.

We observed coexistence of ordered and disordered lipid domains both in the intact viral envelope and in liposomes prepared from viral lipids. It is notable that the fraction of ordered domains in both membrane preparations is the same over a wide temperature range, which suggests that it is primarily determined by the properties of membrane lipids. Thus proteins may play only a limited role in the phase behavior of lipids in the intact viral envelope. However, they may affect line tension at boundaries between coexisting phases[39].

Reducing cholesterol reversibly increases gel-phase lipids. Influenza virus envelope cholesterol also plays a role in virus entry and infection[40]. It has been hypothesized that influenza hemagglutinin concentrates by partitioning into lipid raft microdomains, thus reaching densities needed for the hemagglutinin-mediated fusion of virus infection[41]. Cholesterol melts solid ordered domains into liquid ordered domains and broadens the temperature range of phase transitions of single lipid components. However, as the transition range in viral membranes is already wide due to diversity in polar lipid composition, additional broadening of the temperature range introduced by cholesterol is relatively insignificant. Thus the simple idea that decreasing cholesterol disrupts ordered lipid microdomains should be re-examined. Rather than disrupting all lipid microdomains, lowering envelope cholesterol may convert some liquid domains to solid domains. This solid ordering would diminish trimer mobility, thus preventing aggregation of distant trimers into a fusion complex and thereby inhibiting fusion and infectivity. Given that some trimers would already be close enough to cause infectivity, we predict that cholesterol lowering would only diminish fusion but not stop it, as seen in influenza[41,42] and in human immunodeficiency virus[42].

There are three independent lines of data supporting the notion of solid ordered domains at ambient temperatures. First, in liposomes formed from viral lipids, lipids were confined to areas smaller than the size of the liposomes—results similar to our earlier observations for gel-fluid phase coexistence in SOPC-POPE lipid mixtures[20] and characteristic of solid ordered domains. Second, the rugged edges seen by fluorescence that were observed in supported viral lipid bilayers and in giant unilamellar vesicles suggest that domains are shaped by crystalline packing. Third, methylene resonances that are wider than 1.5 kHz (3 ppm) were assigned to solid ordered lipid phases[20,21]. The presence of such broad components is visible in the first-order spinning sideband of the virus spectrum even at temperatures higher than ambient. Though we may not entirely exclude that those spectra have some contribution from protein resonances, the rapid increase in their intensity with decreasing temperature confirms that they are dominated by contributions from lipids. Taken together, this is strong evidence for the presence of s_o. We speculate that s_o phase formation is related to the high PE content of viral envelopes (**Supplementary Fig. 5** and **Supplementary Table 2** online) as PE has low affinity for cholesterol[24,43,44] and high gel-fluid phase transition temperatures.

At physiological temperature and higher, there is little physical evidence by MAS NMR for ordered lipids. Accordingly, phosphorous NMR spectroscopy of lipid extracts suggests onset of nonbilayer phase formation in viral lipid extracts at temperatures slightly above the temperature of apparent completion of ordered phases melting (**Supplementary Fig. 6** online). Our assay for the chief function of the object, fusion to cell membranes, continues unabated without detectable ordered lipid in the host or target membrane. Thus the study of phase properties of complex, biologically relevant lipid mixtures must be done at the appropriate temperatures. The reason that the viral envelope lipid composition is set to be near an apparent lipid phase boundary with respect to temperature remains unclear. It may be instructive to return to the finding[3] that the lipid composition of the influenza virus is quite different from that of a rhabdovirus that buds from the same cells—vesicular stomatitis virus (VSV). Both of these viruses are enveloped and both bud from the plasma membrane, albeit from different locations. The difference in location relates to their mode of host-to-host transmission: apical budding for aerial transmission of influenza, and serosal budding for transmission

through animal bite for the pathogenic rhabdovirus species, rabies virus. Virus would be at room temperature during aerial transmission but not during transmission by animal bite; the ordered phases we documented here may be important for stability. Indeed, a recent report shows that airborne transmission of influenza virus by guinea pigs is increased at lower temperatures[45], a result predicted by our proposal that the progressive ordering of lipids (demonstrated here) by lower temperatures is important during the low-temperature stages of the influenza life cycle.

METHODS

Sample preparation. All lipids were purchased from Avanti Polar Lipids. Methyl-β-cyclodextrin was purchased from Sigma, and octylglucoside was purchased from Calbiochem. All chemicals used were at least reagent grade.

Influenza virus A X-31, A/Aichi/68 was grown in pathogen-free eggs purchased from CBT Farms and purified according to standard protocols[46]. Egg-grown influenza virus A/2/Japan/305/57 was purchased from SPAFAS. Non-aggregated virus particles were segregated by gel filtration on a PD-10 desalting column (Amersham Biosciences) packed with sephadex G-25. Virus purity was assessed by SDS-PAGE. The fraction of viral proteins in the purified virus comprised at least 95% of the total protein. Fusogenic activity of viruses was confirmed by a lipid-mixing assay based on fluorescence dequenching of R_{18}-labeled virus upon fusion with RBC ghosts[47]. Infectivity of the viruses was confirmed by a plaque-forming assay. Allantoic membranes from embryonated chicken eggs were collected in parallel to harvesting of virus. For sample preparation, virus was pelleted by centrifugation at 25,000 r.p.m. in an SW28 rotor (Beckman Coulter) for 2 h and resuspended in NTE buffer (100 mM NaCl, 10 mM Tris-HCl, 1 mM EDTA, pD 7.4 in ^2H_2O). From 2 to 4 mg of viral particles were separated from extra buffer by centrifugation and transferred to a 4-mm zirconia rotor with a Kel-F spinner cap and Kel-F insert with an 11-μl spherical volume (Bruker Spectrospin Inc.).

The protocol for altering cholesterol content of viral membranes by methyl-β-cyclodextrin was adapted from previous studies[48]. Lipids were extracted from the same virus preparation as used for NMR experiments, according to procedures described previously[49]. Solvents were removed from lipid extracts in a stream of nitrogen gas while rotating the glass tube to form a thin lipid film, followed by drying in vacuum. Multilamellar vesicle samples were prepared by washing the lipid film with 60 °C ^2H_2O-based buffer (10 mM PIPES, pH 7.4, 100 mM NaCl and 50 μM DTPA in ^2H_2O) and transferring vesicles to the MAS rotor by centrifugation. 11 μl of sample contained 2–4 mg of viral lipids.

The virosome preparation procedure was modified from refs. 27,50. Viral particles were solubilized in 45 mM octylglycoside (**9**) at room temperature. The fraction of mixed micelles was separated from the nonsolubilized fraction by centrifugation. The nonsolubilized pellet consisted of matrix proteins and nucleic acids. The content of phospholipids and cholesterol in the nonsolubilized pellet was below sensitivity of standard biochemical assays (phosphate assay and Amplex Red cholesterol assay (Invitrogen)). Viral lipids and membrane proteins were reconstituted into virosomes by rapid dilution below the critical micelle concentration (c.m.c.), to 5 mM, followed by detergent (**9**) removal by dialysis. The average size of virosomes was 105 nm, as determined by dynamic light scattering using Coulter N4Plus particle sizer (Beckman Coulter Inc.). The average size of the intact viruses determined by the same approach was 150 nm.

NMR measurements. ^{1}H MAS NMR experiments were carried out on a Bruker DMX500 spectrometer, equipped with a widebore 11.7 Tesla magnet, a BVT-2000 variable temperature accessory, a MAS control unit and a variable temperature PFG-MAS probe for 4-mm rotors with a gradient oriented at the magic angle (Bruker Spectrospin, Inc.). ^{1}H NMR spectra were recorded at 500.13 MHz, a MAS frequency of 10 kHz and a spectral width of 50 kHz, which covered the spectral centerband and the two first spinning sidebands. Temperature calibration was performed as previously reported[20]. Assignments of ^{1}H MAS NMR resonances of lipid membranes in the liquid disordered state followed the reported assignment of lipid resonances in organic solvent[20].

Lipid diffusion experiments by ^{1}H MAS NMR with application of pulsed magnetic field gradients were performed at a spinning frequency of 10 kHz, as described previously[25] and recapped briefly in the **Supplementary Methods** online.

Fluorescence microscopy. Domain organization in viral lipid membranes was studied by epifluorescence using an Axiovert 25 microscope (Carl Zeiss, Jena) with 32× dry objective. Giant unilamellar vesicles from viral lipid mixtures were prepared by electroformation[30]. 5–10 μl extracted viral lipid in chloroform (1 mg ml^{-1}) containing 1 mol % of rhodamine-DOPE or Texas Red–DPPE (Molecular Probes) were spread with a glass rod on the conducting side of an indium tin oxide–coated (ITO) slide (SPI Supplies) until the solvent evaporated. Remaining traces of solvent were removed by exposure to vacuum for 1 h. The ITO slide was covered with a second conducting slide separated from the first one by a spacer with a thickness of 1.5 mm. The assembly was placed onto a temperature-controlled microscope stage set to 50 °C. After filling the space between the conducting slides with distilled water, some uni- and multilamellar vesicles were observed. An AC field with an amplitude of 3 V and a frequency of 10 Hz from a sine wave AC generator (Wavetek model 183) was applied to the ITO slides for 30 min while we observed formation of vesicles through the microscope. The procedure resulted in formation of an increased fraction of giant unilamellar vesicles floating in the water or attached to the ITO surface.

Membrane fusion. Virus labeled with R18 at self-quenching concentration was mixed with RBC membranes and incubated for 5 min for temperature equilibration. Fusion was triggered by pH adjustment (to pH 5) and monitored by growth of fluorescence due to probe dequenching; 100% of fusion was assigned to complete dequenching observed upon membrane solubilization with 1% Triton-100.

Note: Supplementary information and chemical compound information is available on the Nature Chemical Biology website.

ACKNOWLEDGMENTS

This work was supported by funding from the intramural research programs of the National Institute of Child Health and Human Development and the National Institute on Alcohol Abuse and Alcoholism, US National Institutes of Health. We thank L. Chernomordik and E. Leikina for conducting the experiments on content mixing.

AUTHOR CONTRIBUTIONS

I.V.P., K.G. and J.Z. designed research, analyzed data and wrote the paper. I.V.P. and L.B. performed research.

Published online at http://www.nature.com/naturechemicalbiology
Reprints and permissions information is available online at http://npg.nature.com/reprintsandpermissions

1. Lenard, J. & Compans, R.W. The membrane structure of lipid-containing viruses. *Biochim. Biophys. Acta* **344**, 51–94 (1974).
2. Pessin, J.E. & Glaser, M. Budding of Rous sarcoma virus and vesicular stomatitis virus from localized lipid regions in the plasma membrane of chicken embryo fibroblasts. *J. Biol. Chem.* **255**, 9044–9050 (1980).
3. van Meer, G. & Simons, K. Viruses budding from either the apical or the basolateral plasma-membrane domain of Mdck cells have unique phospholipid compositions. *EMBO J.* **1**, 847–852 (1982).
4. Blom, T.S. *et al.* Mass spectrometric analysis reveals an increase in plasma membrane polyunsaturated phospholipid species upon cellular cholesterol loading. *Biochemistry* **40**, 14635–14644 (2001).
5. Ipsen, J.H., Karlstrom, G., Mouritsen, O.G., Wennerstrom, H. & Zuckermann, M.J. Phase equilibria in the phosphatidylcholine-cholesterol system. *Biochim. Biophys. Acta* **905**, 162–172 (1987).
6. Brown, D.A. & London, E. Structure and origin of ordered lipid domains in biological membranes. *J. Membr. Biol.* **164**, 103–114 (1998).
7. Simons, K. & Ikonen, E. Functional rafts in cell membranes. *Nature* **387**, 569–572 (1997).
8. Lichtenberg, D., Goni, F.M. & Heerklotz, H. Detergent-resistant membranes should not be identified with membrane rafts. *Trends Biochem. Sci.* **30**, 430–436 (2005).
9. Jacobson, K., Mouritsen, O.G. & Anderson, R.G.W. Lipid rafts: at a crossroad between cell biology and physics. *Nat. Cell Biol.* **9**, 7–14 (2007).
10. Sefton, B.M. & Gaffney, B.J. Effect of viral proteins on fluidity of membrane lipids in Sindbis virus. *J. Mol. Biol.* **90**, 343–358 (1974).

11. Landsberger, F.R. & Compans, R.W. Effect of membrane-protein on lipid bilayer structure - spin-label electron-spin resonance study of vesicular stomatitis-virus. *Biochemistry* **15**, 2356–2360 (1976).
12. Landsberger, F.R., Lenard, J., Paxton, J. & Compans, R.W. Spin-label electron spin resonance study of lipid-containing membrane of influenza virus. *Proc. Natl. Acad. Sci. USA* **68**, 2579–2583 (1971).
13. Scheiffele, P., Rietveld, A., Wilk, T. & Simons, K. Influenza viruses select ordered lipid domains during budding from the plasma membrane. *J. Biol. Chem.* **274**, 2038–2044 (1999).
14. Bukrinskaya, A.G., Molotkovsky, J.G., Vodovozova, E.L., Manevich, Y.M. & Bergelson, L.D. The molecular-organization of the influenza-virus surface - studies using photoreactive and fluorescent labeled phospholipid probes. *Biochim. Biophys. Acta* **897**, 285–292 (1987).
15. Lenard, J. Virus envelopes and plasma-membranes. *Annu. Rev. Biophys. Bioeng.* **7**, 139–165 (1978).
16. Hess, S.T. *et al.* Quantitative electron microscopy and fluorescence spectroscopy of the membrane distribution of influenza hemagglutinin. *J. Cell Biol.* **169**, 965–976 (2005).
17. Dietrich, C. *et al.* Lipid rafts reconstituted in model membranes. *Biophys. J.* **80**, 1417–1428 (2001).
18. Veatch, S.L. & Keller, S.L. Separation of liquid phases in giant vesicles of ternary mixtures of phospholipids and cholesterol. *Biophys. J.* **85**, 3074–3083 (2003).
19. Baumgart, T., Hess, S.T. & Webb, W.W. Imaging coexisting fluid domains in biomembrane models coupling curvature and line tension. *Nature* **425**, 821–824 (2003).
20. Polozov, I.V. & Gawrisch, K. Domains in binary SOPC/POPE lipid mixtures studied by pulsed field gradient ^{1}H MAS NMR. *Biophys. J.* **87**, 1741–1751 (2004).
21. Polozov, I.V. & Gawrisch, K. Characterization of the liquid-ordered state by proton MAS NMR. *Biophys. J.* **90**, 2051–2061 (2006).
22. Veatch, S.L., Polozov, I.V., Gawrisch, K. & Keller, S.L. Liquid domains in vesicles investigated by NMR and fluorescence microscopy. *Biophys. J.* **86**, 2910–2922 (2004).
23. Oldfield, E., Bowers, J.L. & Forbes, J. High-resolution proton and carbon-13 NMR of membranes: why sonicate? *Biochemistry* **26**, 6919–6923 (1987).
24. Huster, D., Arnold, K. & Gawrisch, K. Influence of docosahexaenoic acid and cholesterol on lateral lipid organization in phospholipid mixtures. *Biochemistry* **37**, 17299–17308 (1998).
25. Gaede, H.C. & Gawrisch, K. Lateral diffusion rates of lipid, water, and a hydrophobic drug in a multilamellar liposome. *Biophys. J.* **85**, 1734–1740 (2003).
26. Rothman, J.E., Tsai, D.K., Dawidowicz, E.A. & Lenard, J. Transbilayer phospholipid asymmetry and its maintenance in membrane of influenza-virus. *Biochemistry* **15**, 2361–2370 (1976).
27. Stegmann, T. *et al.* Functional reconstitution of influenza-virus envelopes. *EMBO J.* **6**, 2651–2659 (1987).
28. Filippov, A., Oradd, G. & Lindblom, G. The effect of cholesterol on the lateral diffusion of phospholipids in oriented bilayers. *Biophys. J.* **84**, 3079–3086 (2003).
29. Scheidt, H.A., Huster, D. & Gawrisch, K. Diffusion of cholesterol and its precursors in lipid membranes studied by ^{1}H PFG MAS NMR. *Biophys. J.* **89**, 2504–2512 (2005).
30. Hac, A.E., Seeger, H.M., Fidorra, M. & Heimburg, T. Diffusion in two-component lipid membranes—a fluorescence correlation spectroscopy and Monte Carlo simulation study. *Biophys. J.* **88**, 317–333 (2005).
31. Harris, A. *et al.* Influenza virus pleiomorphy characterized by cryoelectron tomography. *Proc. Natl. Acad. Sci. USA* **103**, 19123–19127 (2006).
32. Hess, S.T. *et al.* Dynamic clustered distribution of hemagglutinin resolved at 40 nm in living cell membranes discriminates between raft theories. *Proc. Natl. Acad. Sci. USA* **104**, 17370–17375 (2007).
33. Filippov, A., Oradd, G. & Lindblom, G. Sphingomyelin structure influences the lateral diffusion and raft formation in lipid bilayers. *Biophys. J.* **90**, 2086–2092 (2006).
34. Koynova, R. & Caffrey, M. Phases and phase-transitions of the sphingolipids. *Biochim. Biophys. Acta* **1255**, 213–236 (1995).
35. Clarke, J.A., Heron, A.J., Seddon, J.M. & Law, R.V. The diversity of the liquid ordered (L-o) phase of phosphatidylcholine/cholesterol membranes: a variable temperature multinuclear solid-state NMR and X-ray diffraction study. *Biophys. J.* **90**, 2383–2393 (2006).
36. McMullen, T.P. & McElhaney, R.N. New aspects of the interaction of cholesterol with dipalmitoylphosphatidylcholine bilayers as revealed by high-sensitivity differential scanning calorimetry. *Biochim. Biophys. Acta* **1234**, 90–98 (1995).
37. Polozov, I.V., Molotkovsky, J.G. & Bergelson, L.D. Anthrylvinyl-labeled phospholipids as membrane probes - the phosphatidylcholine-phosphatidylethanolamine system. *Chem. Phys. Lipids* **69**, 209–218 (1994).
38. Heberle, F.A., Buboltz, J.T., Stringer, D. & Feigenson, G.W. Fluorescence methods to detect phase boundaries in lipid bilayer mixtures. *Biochim. Biophys. Acta* **1746**, 186–192 (2005).
39. Kuzmin, P.I., Akimov, S.A., Chizmadzhev, Y.A., Zimmerberg, J. & Cohen, F.S. Line tension and interaction energies of membrane rafts calculated from lipid splay and tilt. *Biophys. J.* **88**, 1120–1133 (2005).
40. Sun, X. & Whittaker, G.R. Role for influenza virus envelope cholesterol in virus entry and infection. *J. Virol.* **77**, 12543–12551 (2003).
41. Takeda, M., Leser, G.P., Russell, C.J. & Lamb, R.A. Influenza virus hemagglutinin concentrates in lipid raft microdomains for efficient viral fusion. *Proc. Natl. Acad. Sci. USA* **100**, 14610–14617 (2003).
42. Campbell, S. *et al.* The raft-promoting property of virion-associated cholesterol, but not the presence of virion-associated Brij 98 rafts, is a determinant of human immunodeficiency virus type 1 infectivity. *J. Virol.* **78**, 10556–10565 (2004).
43. Silvius, J.R. Role of cholesterol in lipid raft formation: lessons from lipid model systems. *Biochim. Biophys. Acta* **1610**, 174–183 (2003).
44. Niu, S.L. & Litman, B.J. Determination of membrane cholesterol partition coefficient using a lipid vesicle-cyclodextrin binary system: effect of phospholipid acyl chain unsaturation and headgroup composition. *Biophys. J.* **83**, 3408–3415 (2002).
45. Lowen, A.C., Mubareka, S., Steel, J. & Palese, P. Influenza virus transmission is dependent on relative humidity and temperature. *PLoS Pathog.* **3**, 1470–1476 (2007).
46. Paterson, R.G. & Lamb, R.A. *Molecular Virology: a Practical Approach* (eds. Davidson, A. & Elliott, R.M.) 35–73 (IRL Oxford University Press, Oxford, 1993).
47. Hoekstra, D., Deboer, T., Klappe, K. & Wilschut, J. Fluorescence method for measuring the kinetics of fusion between biological membranes. *Biochemistry* **23**, 5675–5681 (1984).
48. Klein, U., Gimpl, G. & Fahrenholz, F. Alteration of the myometrial plasma-membrane cholesterol content with beta-cyclodextrin modulates the binding-affinity of the oxytocin receptor. *Biochemistry* **34**, 13784–13793 (1995).
49. Folch, J., Lees, M. & Sloane-Stanley, G.H. A simple method for the isolation and purification of total lipides from animal tissues. *J. Biol. Chem.* **226**, 497–509 (1957).
50. Metsikko, K., Vanmeer, G. & Simons, K. Reconstitution of the fusogenic activity of vesicular stomatitis-virus. *EMBO J.* **5**, 3429–3435 (1986).